

Supplemental Information

Novel AAV44.9-Based Vectors Display Exceptional Characteristics for Retinal Gene Therapy

Sanford L. Boye, Shreyasi Choudhury, Sean Crosson, Giovanni Di Pasquale, Sandra Afione, Russell Mellen, Victoria Makal, Kaitlyn R. Calabro, Diego Fajardo, James Peterson, Hangning Zhang, Matthew T. Leahy, Colin K. Jennings, John A. Chiorini, Ryan F. Boyd, and Shannon E. Boye

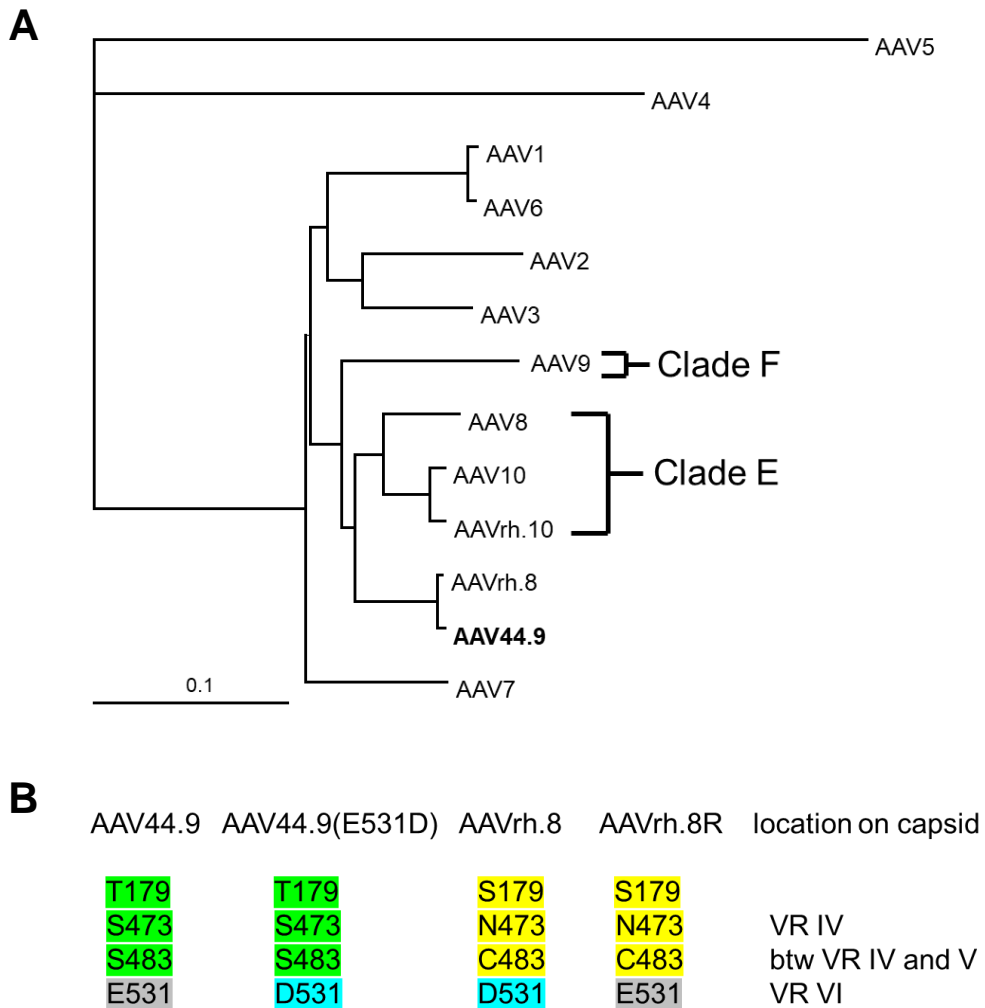


Figure S1. Phylogeny of select AAVs based on VP1 amino acid sequences using neighbor-joining method (A). Specific amino acid substitutions for AAV44.9 and related variants and location on capsid (B). Color denotes residue is shared across different capsids. VR denotes variable loop on capsid surface, IV, V and VI are roman numerals.

Vector Prep	Scale (cell surface area)	Vector Concentration (vg/mL)	Total Vector Yield (vg)	Yield/cell (vg/cell)
scAAV44.9-smCBA-mCherry	1272 cm ²	2.16E+13	2.81E+12	1.41E+04
scAAV44.9-smCBA-mCherry	1272 cm ²	1.59E+13	2.07E+12	1.04E+04
scAAV44.9(E531D)-smCBA-mCherry	1272 cm ²	1.51E+13	1.96E+12	9.80E+03
scAAV44.9(E531D)-smCBA-mCherry	1272 cm ²	1.06E+13	1.38E+12	6.90E+03
scAAV44.9(E531K)-smCBA-mCherry	1272 cm ²	5.15E+13	1.03E+13	5.15E+04
scAAV44.9(Y733F)-smCBA-mCherry	1272 cm ²	1.90E+13	2.47E+12	1.24E+04
scAAV8(Y733F)-smCBA-mCherry	1272 cm ²	2.59E+12	3.24E+11	1.62E+03
scAAVrh.8-smCBA-mCherry	1272 cm ²	1.98E+13	2.57E+12	1.29E+04
scAAV6-smCBA-mCherry	1272 cm ²	2.99E+12	4.63E+11	2.32E+03
scAAV5-smCBA-mCherry	1272 cm ²	3.82E+13	4.01E+12	2.01E+04
AAV44.9-CBA-GFP	6,360 cm ²	1.41E+13	4.23E+12	4.23E+03
AAV44.9-hGRK1-GFP	6,360 cm ²	1.49E+13	4.47E+12	4.47E+03
AAV44.9(E531D)-hGRK1-GFP	6,360 cm ²	1.60E+13	4.80E+12	4.80E+03
AAV5-hGRK1-GFP	6,360 cm ²	7.63E+12	4.12E+12	4.12E+03
AAV44.9(E531D)-hGRK1-Gucy2e	6,360 cm ²	1.17E+13	4.39E+12	4.39E+03

Table S1. Total yield and concentration of vectors produced via plasmid-based triple transfection. AAV preparations made at the 6,360cm² scale underwent additional step of ion-exchange chromatography purification.

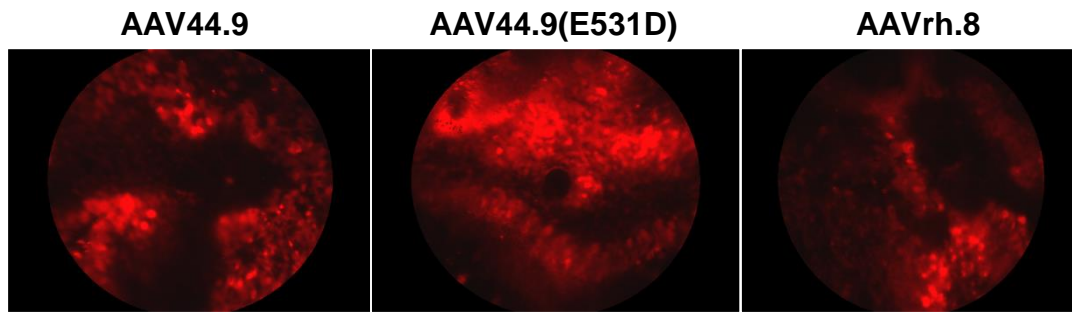


Figure S2. Qualitative analysis of retinal transduction following subretinal injection (SRI) of novel capsid variants. Representative fluorescent fundus images of Nrl-GFP mouse retinas 4 weeks post-SRI with 2×10^8 vgs of AAV44.9, AAV44.9(E531D), or AAVrh.8 vectors containing smCBA-mCherry. Images were captured using identical settings. At this lower dose, AAV44.9(E531D) outperforms both AAV44.9 and AAVrh.8.

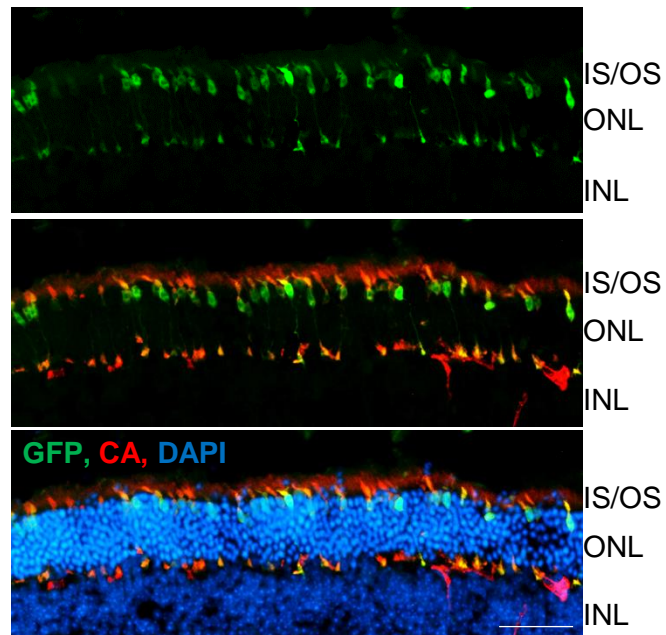


Figure S3. Transduction profile of AAV44.9-IRBP/GNAT2-GFP following SRI in C57BL6J mice. Six weeks post-injection with 2×10^{12} vg/mL, retinal cross sections were stained with an antibody directed against cone arrestin (CA) and counterstained with DAPI. Vector-mediated GFP expression and cone arrestin colocalize indicating this capsid efficiently transduces cone photoreceptors. Scale bar= 50 microns. IS/OS- inner segments/outer segments, ONL- outer nuclear layer, INL- inner nuclear layer.

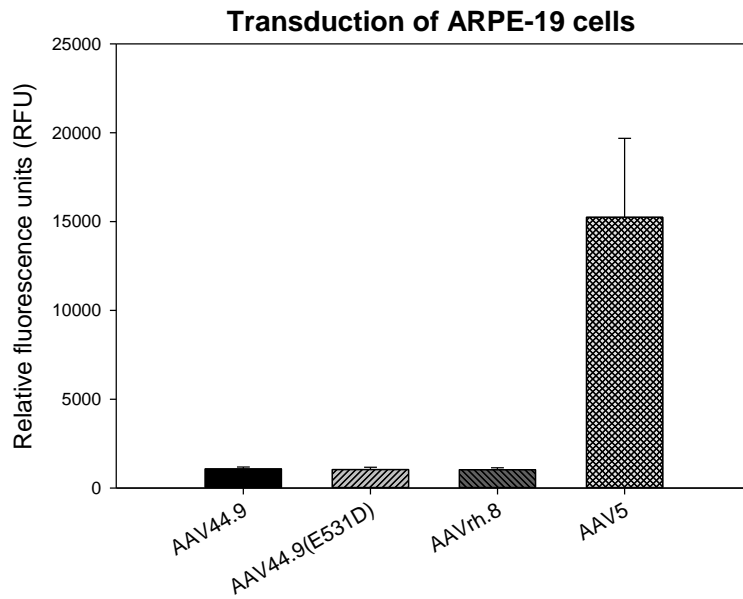


Figure S4. Quantitative analysis of transduction by novel capsid variants *in vitro*. Self-complimentary constructs containing the smCBA promoter driving mCherry were packaged in AAV44.9, AAV44.9(E531D), AAVrh.8, or AAV5. ARPE19 cells were infected with vector at an MOI of 10,000. Three days post-infection, cells were dissociated and flow cytometry used to quantify the relative fluorescence (% mCherry positive cells x fluorescence intensity).

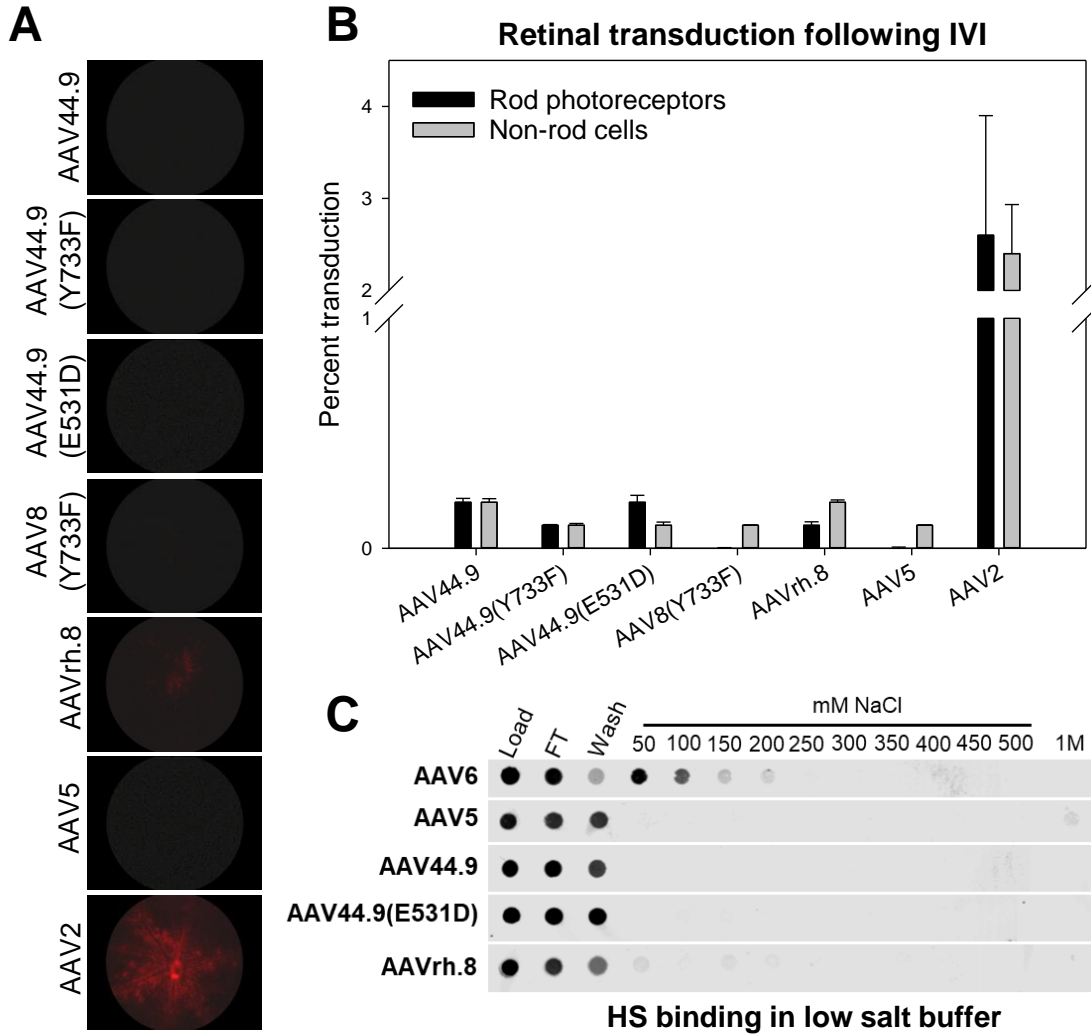


Figure S5. Qualitative (A) and quantitative (B) analysis of retinal transduction following intravitreal injection (IVI) of novel capsid variants. Fundus images of Nrl-GFP mouse retinas 4 weeks post-IVI with 2×10^9 vg of AAV44.9, AAV44.9(Y733F), AAV44.9(E531D), AAVrh.8, AAV8(Y733F), AAV5 or AAV2 (A). Images were captured using identical settings. Similar to benchmark vectors, AAV5 and AAV8(Y733F), AAV44.9 and its derivatives do not efficiently transduce retina following IVI. A closely related capsid, AAVrh.8 also fails to efficiently transduce retina via this route. Flow cytometry was performed on dissociated retinas and the percent rod vs. non-rod retinal transduction by capsids was quantified (B). Heparin binding elution profiles of AAV44.9 and AAV44.9(E531D) capsids relative to AAV6, AAV5 and AAVrh.8 at different salt concentrations (C). Background buffer was lowered to 220mOsm. Salt concentrations presented are in addition to this osmolarity.

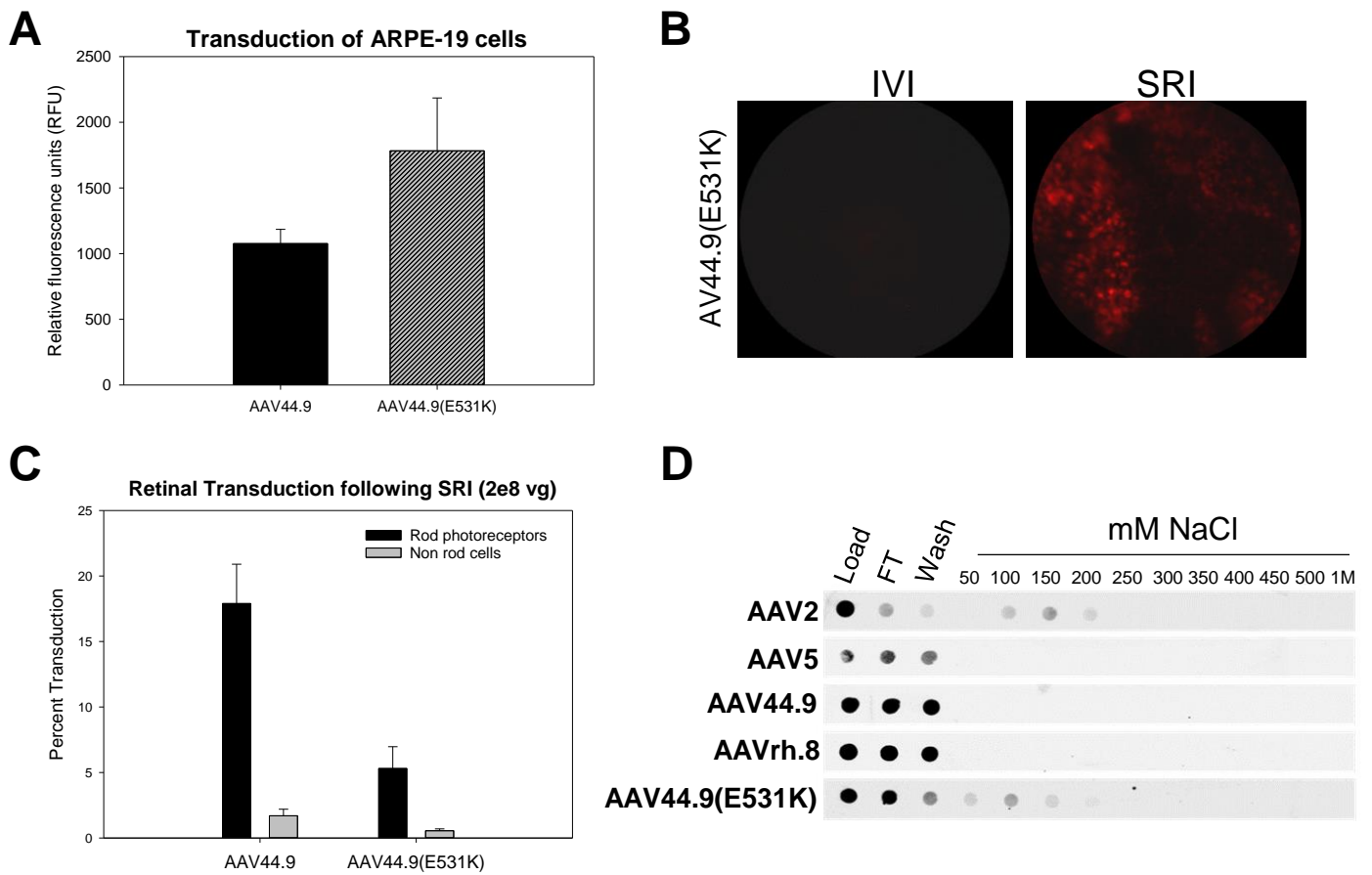


Figure S6. Quantitative analysis of transduction by AAV44.9(E531K) *in vitro*. Self-complementary constructs containing the smCBA promoter driving mCherry were packaged in AAV44.9(E531K), closely related capsids and benchmark AAV5. ARPE19 cells were infected at an MOI of 10,000. Three days post-infection, cells were dissociated and flow cytometry used to quantify relative fluorescence (% mCherry positive cells x fluorescence intensity). Qualitative (B) and quantitative (C) analysis of retinal transduction by AAV44.9(E531K) *in vivo*. Fundus images of Nrl-GFP mouse retinas 4 weeks post-IVI or SRI with 2e8 vgs of AAV44.9(E531K) (B). Images were captured using identical settings. AAV44.9(E531K) does not transduce retina following IVI and only modestly transduces retina following SRI. Flow cytometry was performed on dissociated retinas from subretinally injected mice and the percent rod vs. non-rod retinal transduction by capsids was quantified relative to closely related capsids (C). Heparin binding elution profiles of AAV44.9 and AAV44.9(E531K) capsids relative to AAV2, AAV5 and AAVrh.8 at different salt concentrations (D).

Group #	N	OD	OS	Concentration	Volume/Bleb Location
1	2	n/a	AAV44.9-CBA-GFP	1x10 ¹² vg/mL	60uL/bleb Bleb #1- submacular, Bleb #2- inferior
2	2	n/a	AAV44.9-hGRK1-GFP	1x10 ¹² vg/mL	60uL/bleb Bleb #1- submacular, Bleb #2- inferior
3	1	n/a	AAV5-hGRK1-GFP	1x10 ¹² vg/mL	90 µl, Three 30uL extrafoveal blebs
4	1	n/a	AAV44.9-hGRK1-GFP	1x10 ¹² vg/mL	90 µl, Three 30uL extrafoveal blebs
5	1	AAV44.9-hGRK1-GFP	AAV44.9(E531D)-hGRK1-GFP	1x10 ¹² vg/mL	90 µl, Three 30uL extrafoveal blebs

Table S2. NHP injection details

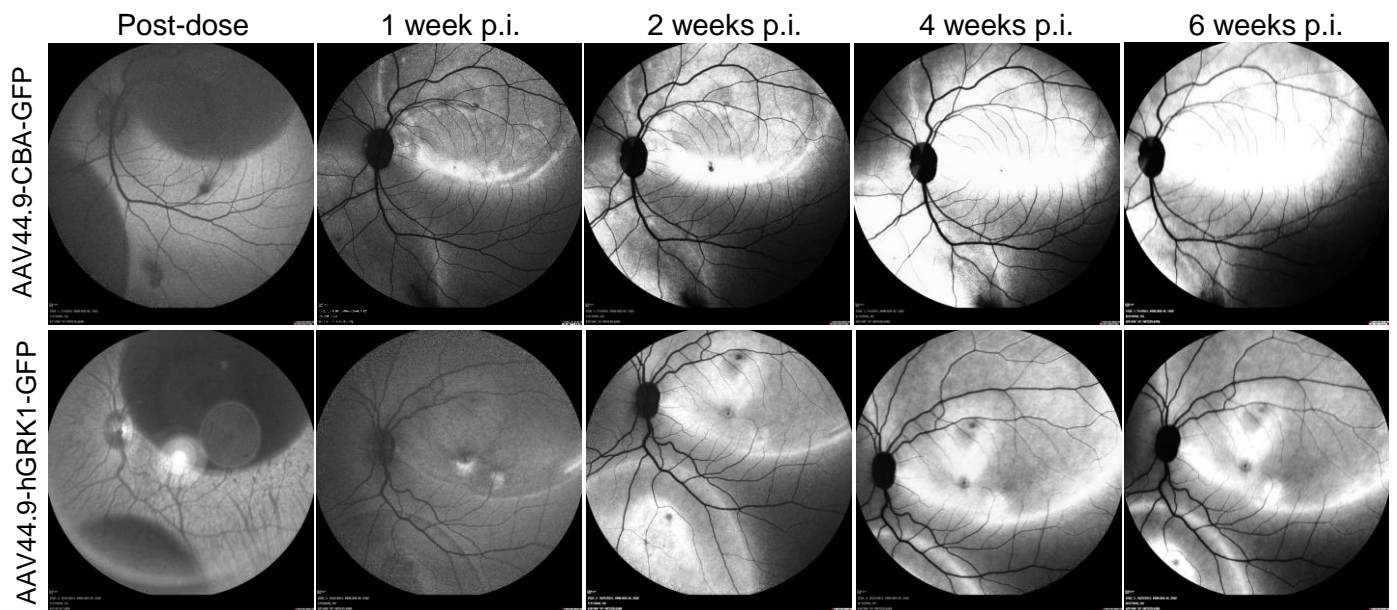
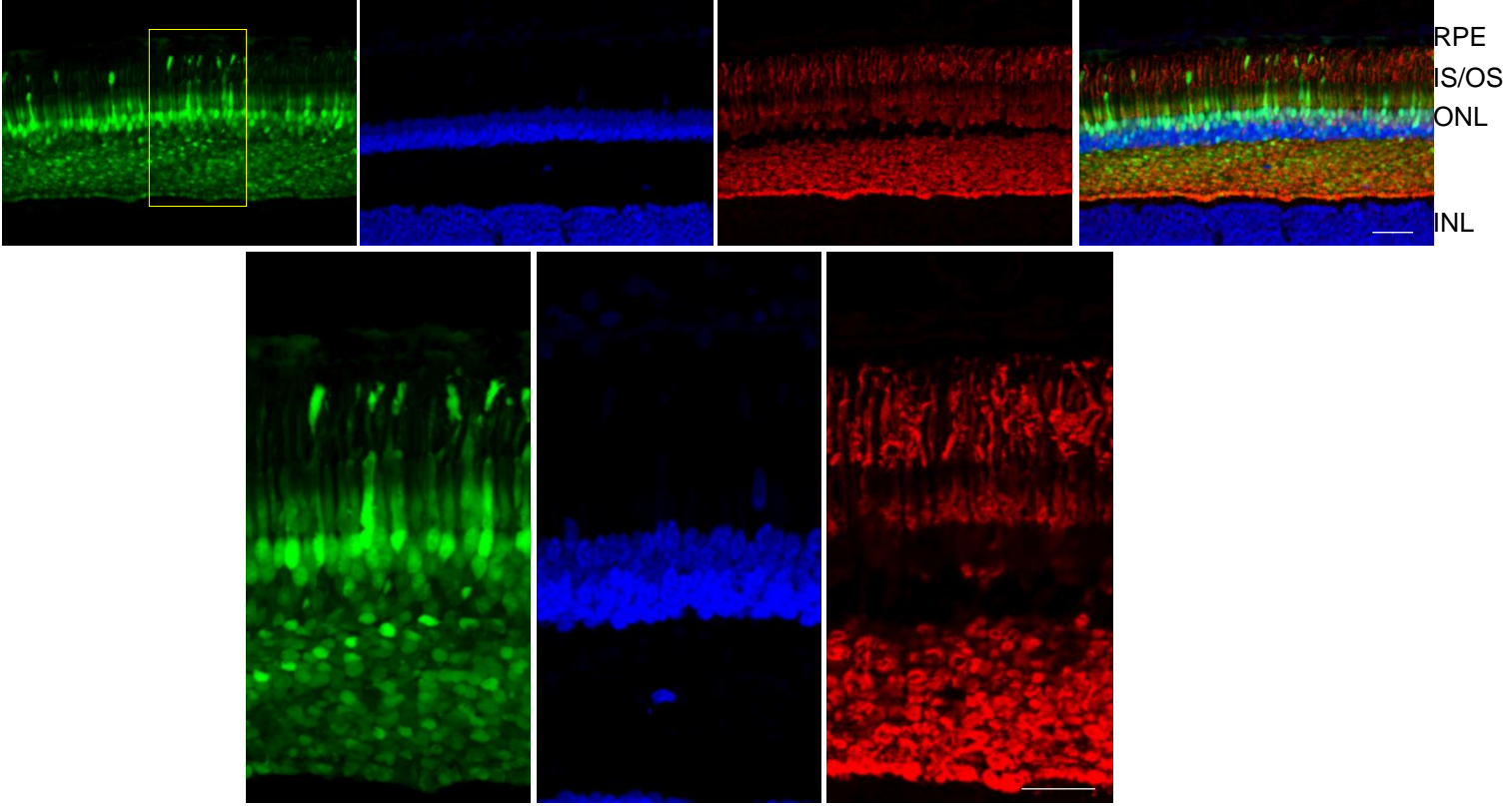


Figure S7. Representative macaque fundus images taken immediately after central and peripheral subretinal injection, then at 1 week, 2 weeks, 4 weeks and 6 weeks post-injection with either AAV44.9-CBA or AAV44.9-hGRK1 vectors driving GFP.

Vector	Bleb Location	Area Analyzed	% cones transduced	% rods transduced
AAV44.9-CBA	submacular	fovea	95%	96%
	peripheral	inferotemporal	100%	95%
AAV44.9-hGRK1	submacular	fovea	97%	81%
	peripheral	temporal	97%	96%
	extrafoveal	fovea	96%	98%
AAV44.9(E531D)-hGRK1	peripheral	temporal	93%	95%
	extrafoveal	fovea	98%	100%
AAV5-hGRK1	peripheral	temporal	89%	92%
	extrafoveal	fovea	0%	0%

Table S3. Summary of cone and rod transduction in subretinally injected macaque, according to bleb location

AAV44.9-CBA-GFP temporal parafovea



AAV44.9-CBA-GFP nasal parafovea

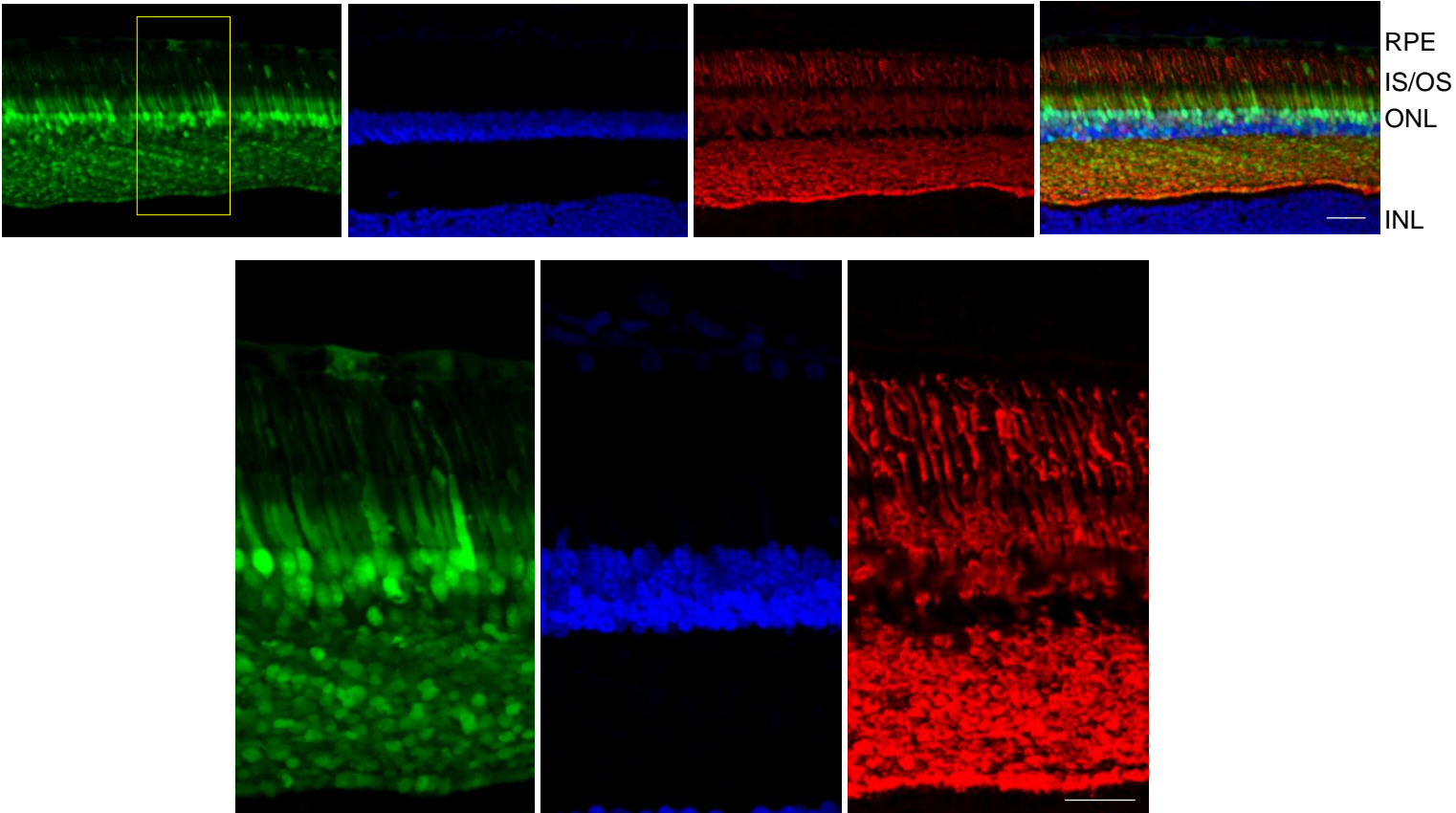


Figure S8. Representative retinal cross sections from the temporal (top) and nasal (bottom) parafovea of eyes that received submacular subretinal injection of AAV44.9-CBA-GFP. Retinas were stained with an antibody raised against cone arrestin (red) and counterstained with DAPI (blue). Scale bars in low mag (20X) images = 40 microns, high mag (40X) images= 20 microns

AAV44.9-hGRK1-GFP

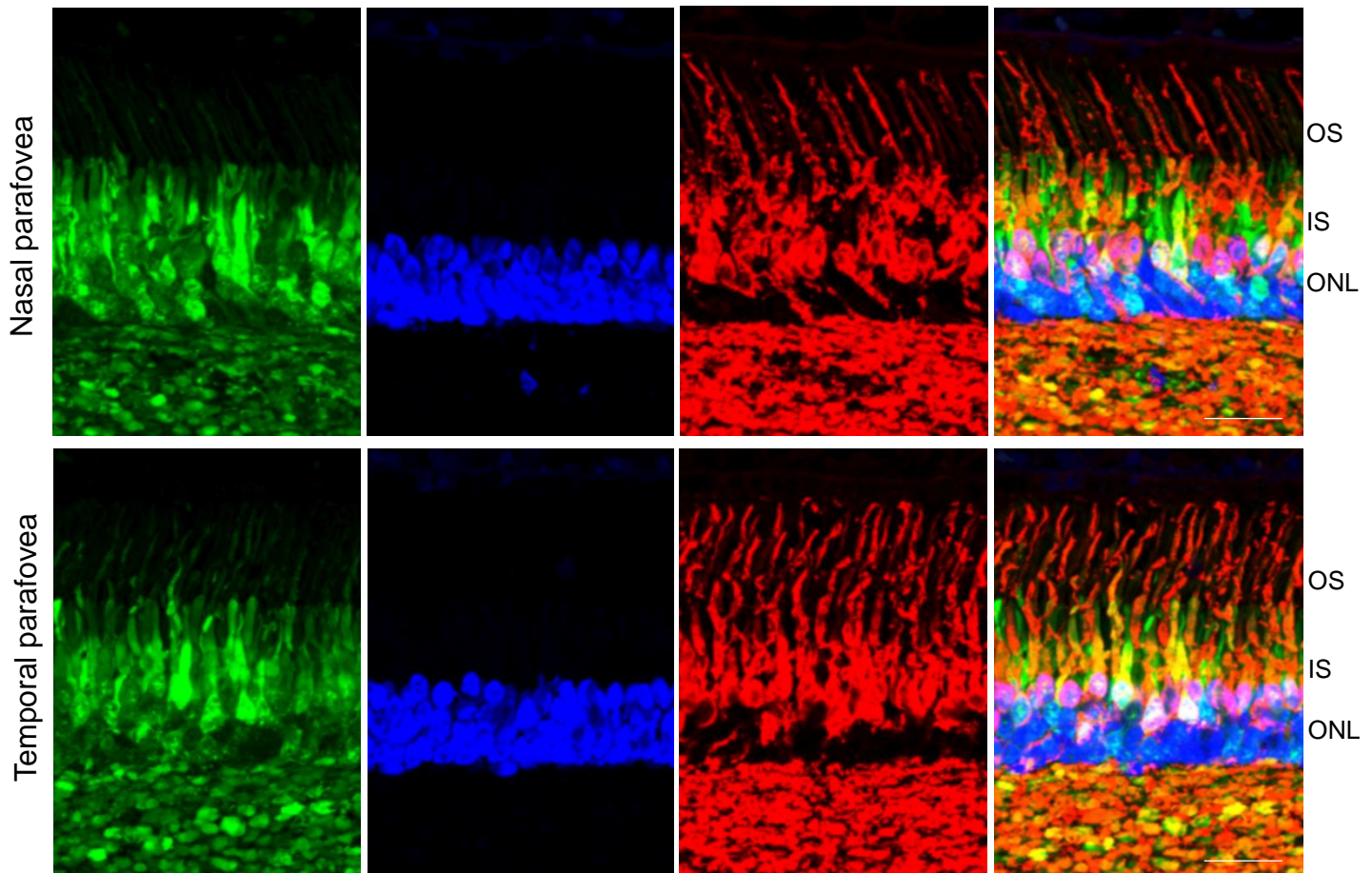


Figure S9. Retinal cross sections from macaque eyes that received submacular subretinal injections (SRI) of AAV44.9-hGRK1-GFP. Sections from the nasal and temporal parafovea were immunostained with an antibody raised against cone arrestin (red) and counter stained with DAPI (blue). GFP expression (green) was present in parafoveal cones (~550 μ M nasal or temporal from the foveal pit) in eyes injected with AAV44.9-hGRK1. Scale bars= 20 microns. IS- inner segments, OS-outer segments, ONL- outer nuclear layer

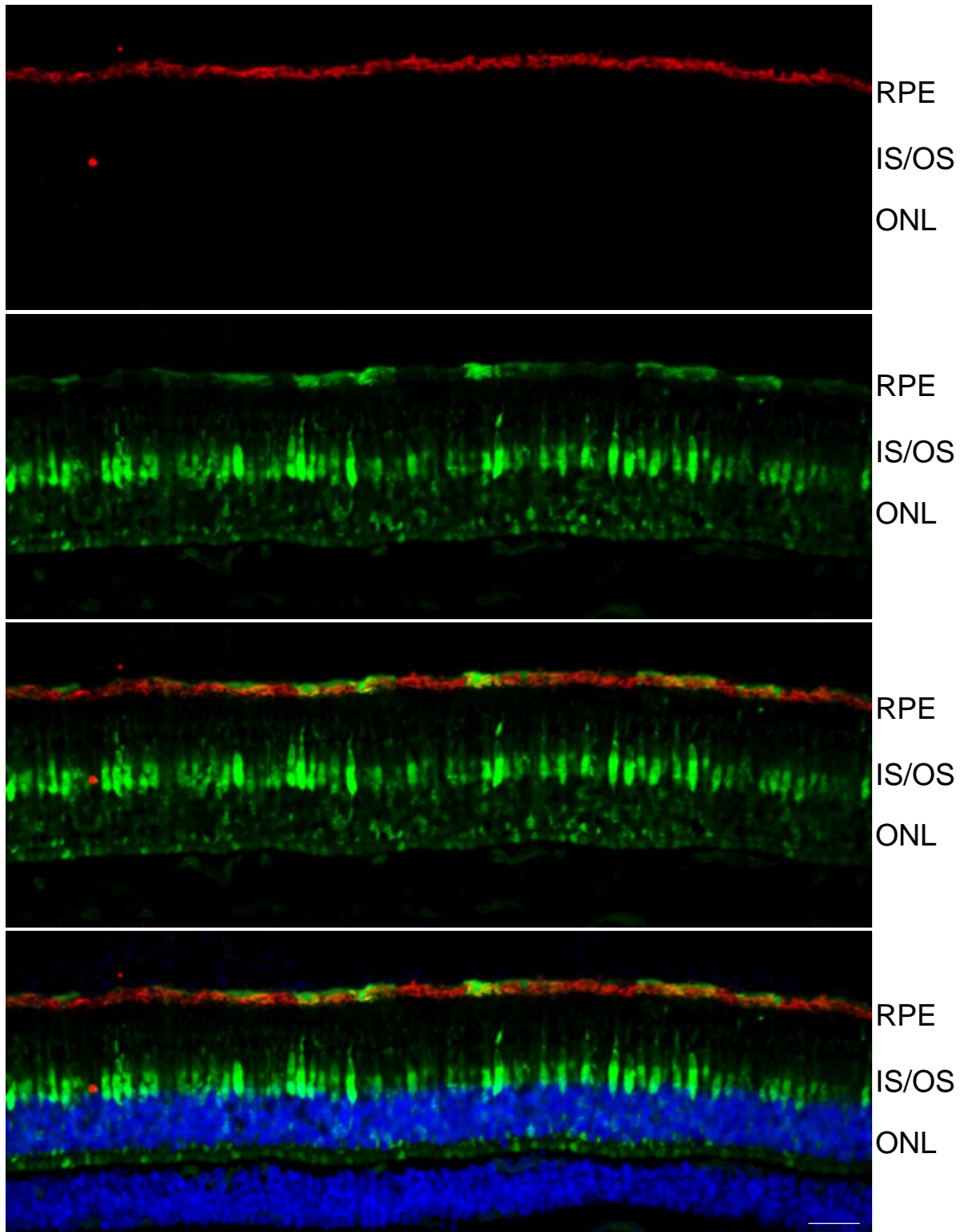


Figure S10. Representative retinal cross section from macaque eye that received subretinal injections (SRI) of AAV44.9-CBA-GFP immunostained with an antibody raised against RPE65 (red) and counter stained with DAPI (blue). 40X image is shown. Scale bar= 40 microns. RPE= retinal pigment epithelium, IS/OS= inner segments/outer segments, ONL= outer nuclear layer. Scale bar= 40 microns

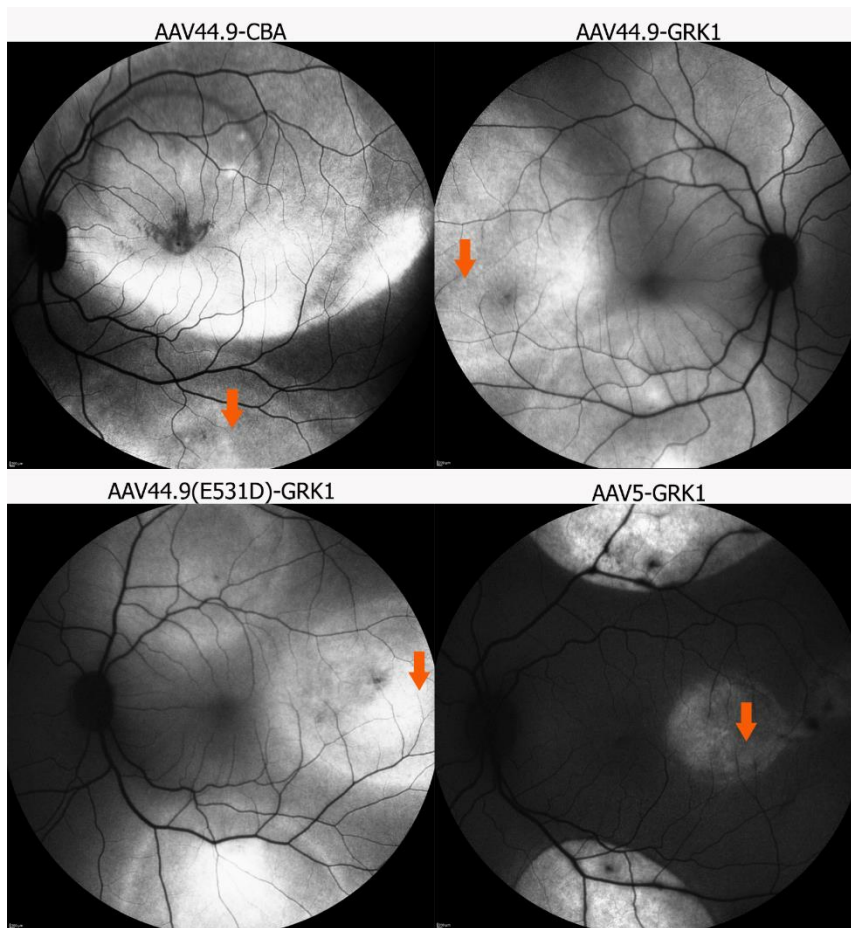


Figure S11. Confocal scanning laser ophthalmoscopy (SLO) images of macaque eyes subretinally injected with AAV44.9-CBA, AAV44.9-hGRK1, AAV44.9(E531D)-hGRK1, or AAV5-hGRK1 vectors. Orange arrows demarcate the locations in peripheral retinas from which cross sectional analyses in Figure 2 was performed.

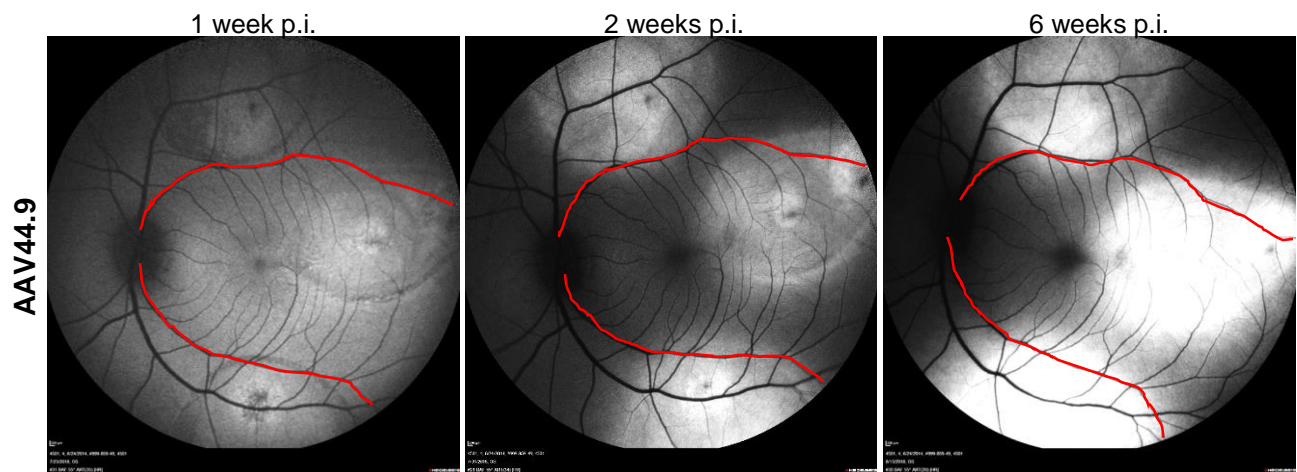


Figure S12. Confocal scanning laser ophthalmoscopy (SLO) images of macaque eyes that received 3 extrafoveal subretinal injections (30 μ L each) of AAV44.9 vector containing hGRK1-GFP (1×10^{12} vg/mL). Each injection was placed approximately 25 degrees away from the foveal pit. Images could not be obtained on the day of dosing, but were captured at 1, 2, and 6 weeks post-injection. Red lines are superimposed on retinal vasculature to serve as landmarks.

AAV44.9-hGRK1-GFP

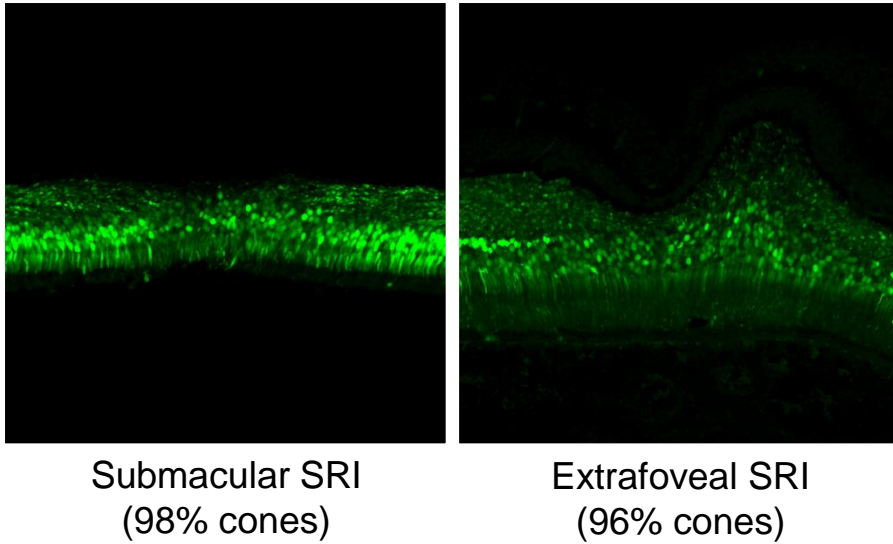


Figure S13. Photoreceptor transduction in the foveal pit of eyes that received either submacular or extrafoveal subretinal injection (SRI) of AAV44.9-hGRK1-GFP. The percent of GFP positive cones in these retinal cross sections, quantified by three blinded observers, was almost identical despite differences in surgical delivery.

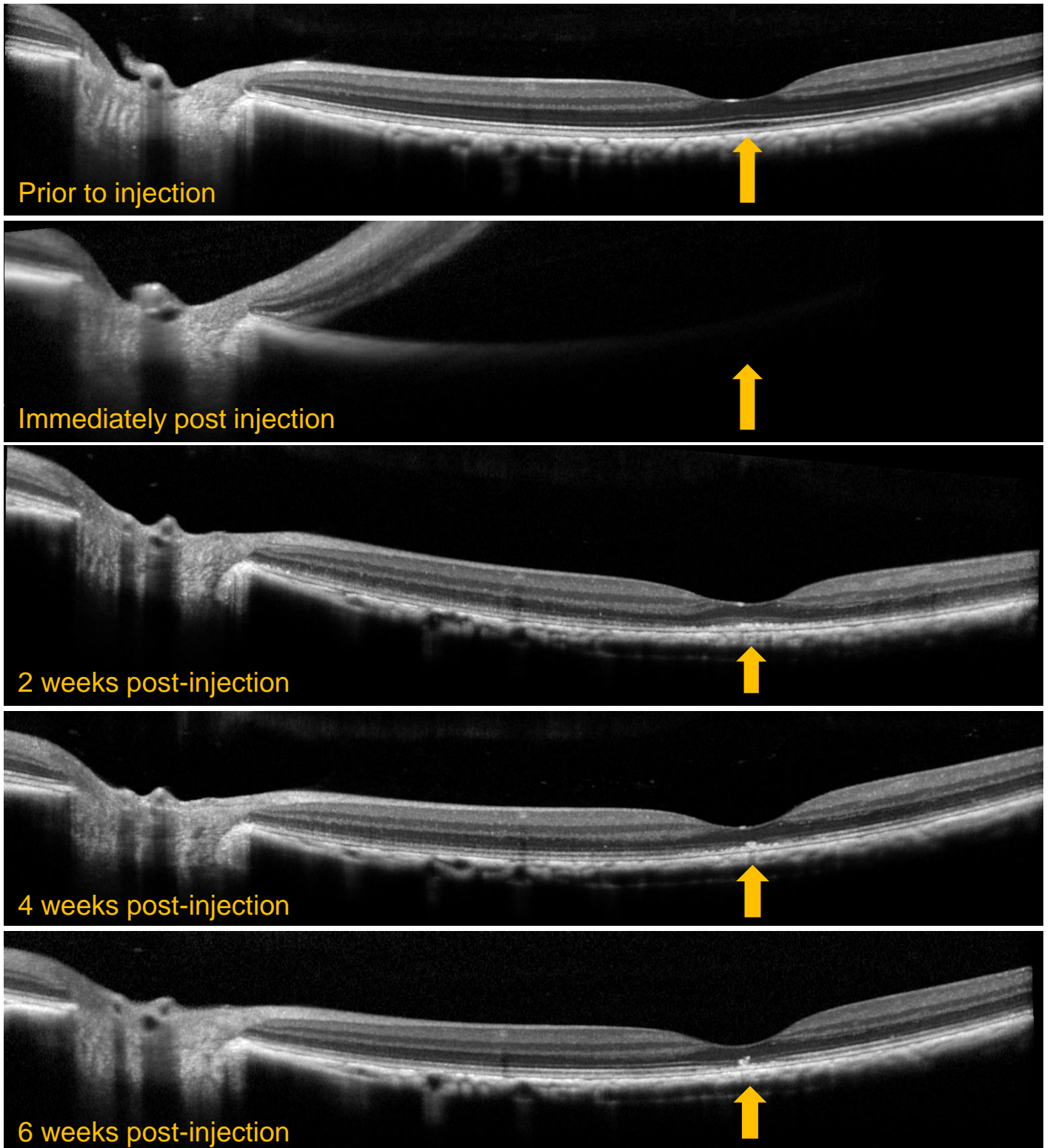


Figure S14. OCT scans from an eye that received a submacular SRI of AAV44.9-hGRK1-GFP. A loss of ellipsoid zone, and foveal bulge are present at 2 weeks post-injection. Structural abnormalities have not resolved by the study's end. Orange arrows demarcate location of foveal pit.

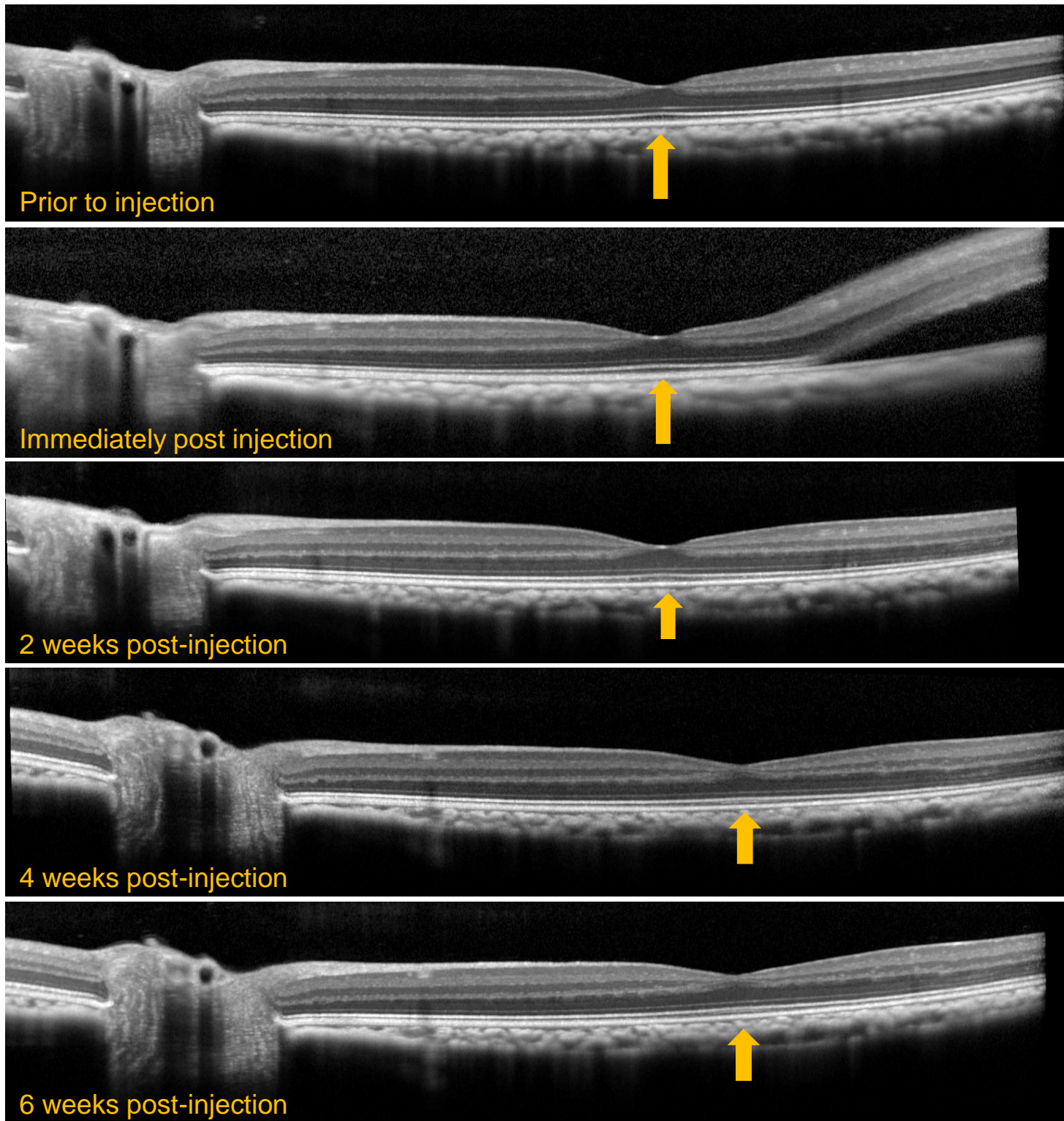


Figure S15. OCT scans from an eye that received a extrafoveal SRI of AAV44.9-hGRK1-GFP. No gross structural changes were observed in the fovea over the course of the study.

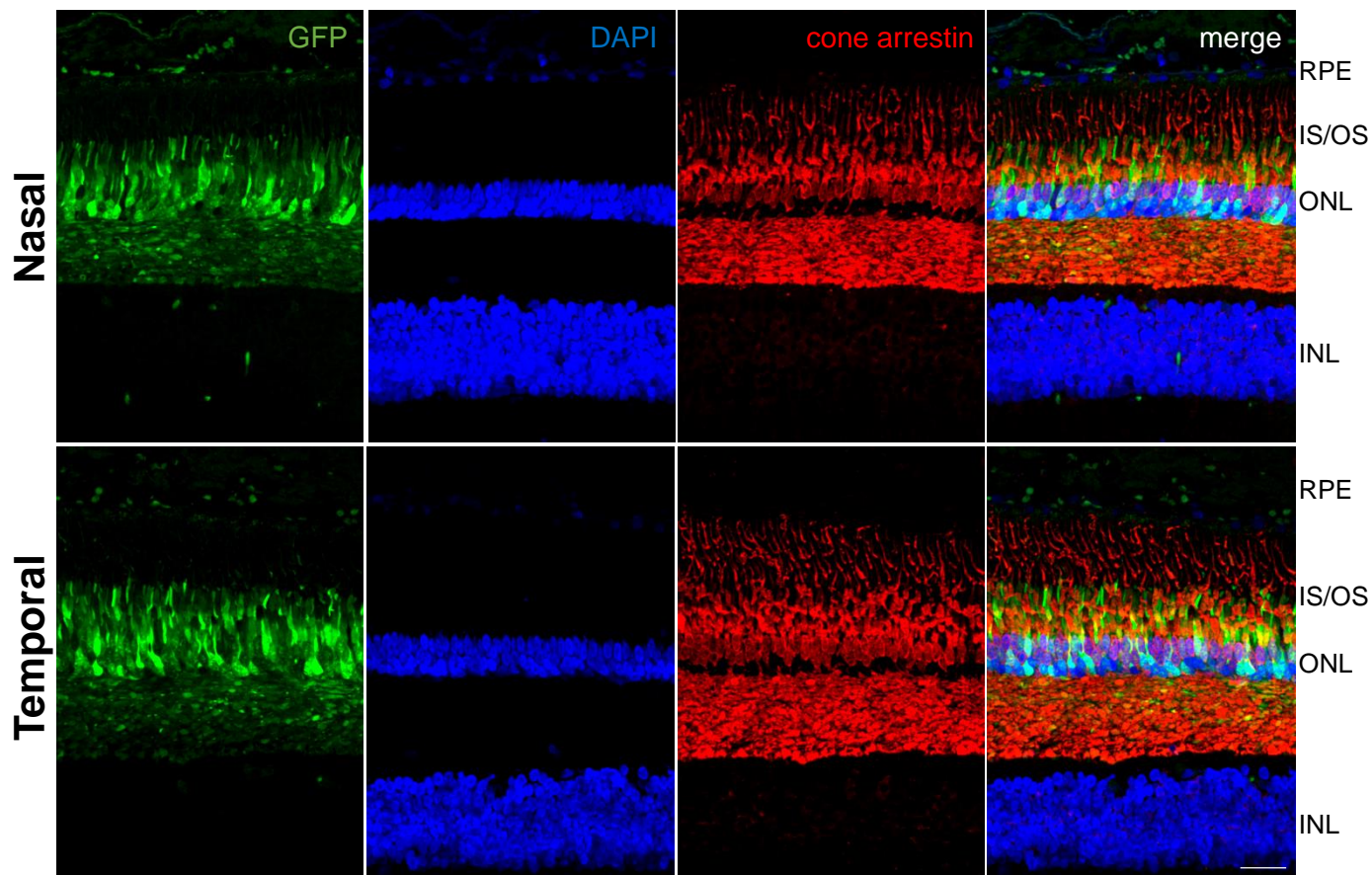


Figure S16. Retinal cross sections from macaque eyes that received extrafoveal subretinal injections (SRI) of AAV44.9(E531D)-hGRK1-GFP immunostained with an antibody raised against cone arrestin (red) and counter stained with DAPI (blue). Nasal and temporal parafoveal cones (~550 microns from foveal pit) express AAV44.9(E531D)- mediated GFP. 40X images are shown. Scale bar= 40 microns. RPE- retinal pigment epithelium, IS/OS- inner segments/outer segments, ONL- outer nuclear layer, INL- inner nuclear layer

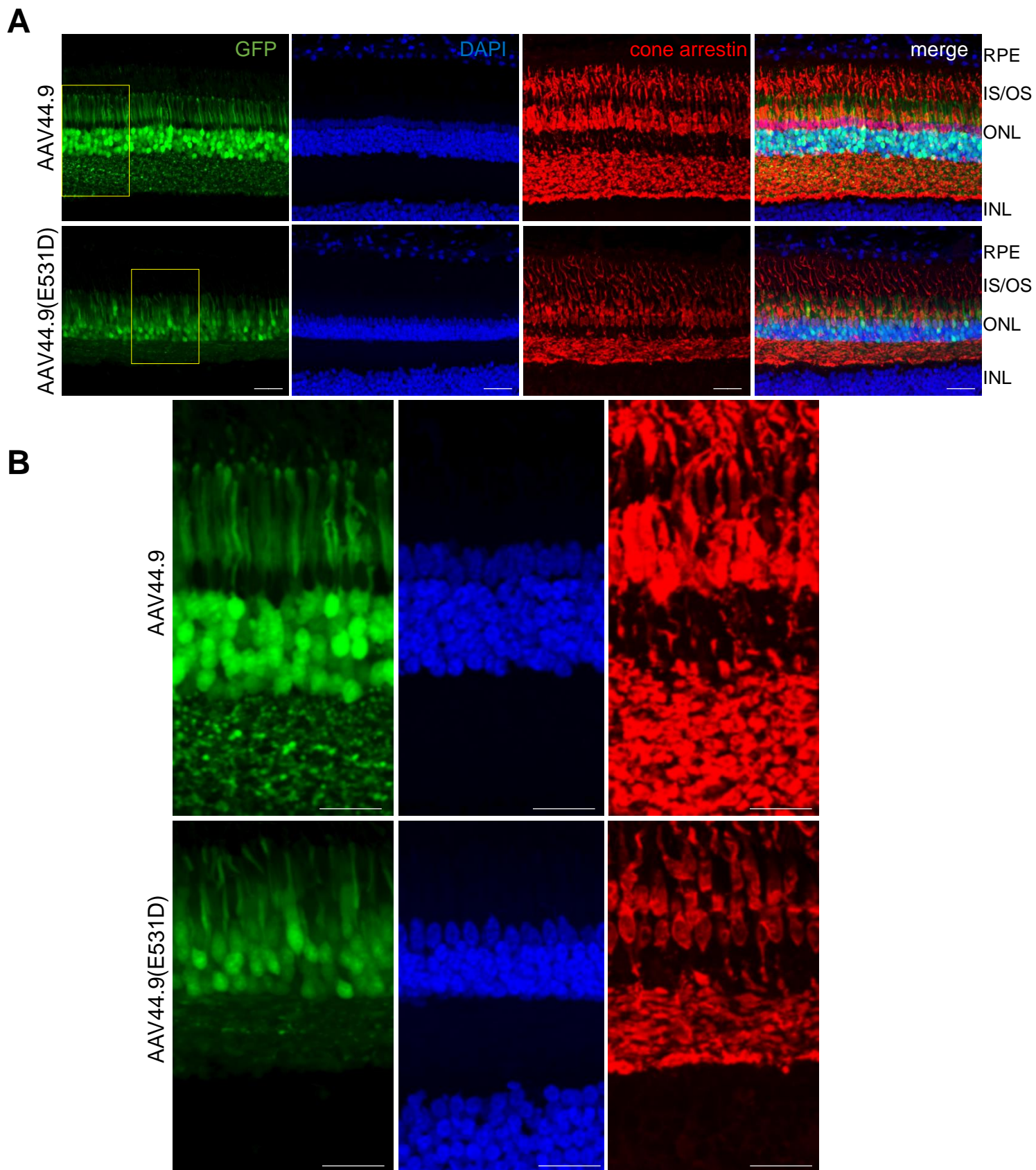


Figure S17. Retinal cross sections from macaque eyes that received extrafoveal subretinal injections (SRI) of AAV44.9-hGRK1-GFP (A,B- top row) or AAV44.9(E531D)-hGRK1-GFP (A,B- bottom row) were immunostained with an antibody raised against cone arrestin (red) and counter stained with DAPI (blue). GFP expression (green) was absent from perifoveal cones ($\sim 1100 \mu\text{M}$ nasal or temporal from the foveal pit) in eyes injected with AAV44.9. In contrast, perifoveal cones efficiently expressed AAV44.9(E531D)-mediated GFP. 20X (A, C) and 40X (C, D) images are shown. Scale bars in A= 40 microns, B= 20 microns. RPE- retinal pigment epithelium, IS/OS- inner segments/outer segments, ONL- outer nuclear layer, INL- inner nuclear layer.